The Photon strength function of ^{58}Fe via the inverse Oslo and shape methods

A. Abbott,[1,2] M. Q. Sorensen,[1,2] A. B. McIntosh,[1] A. Alvarez,[1,3] A. Couture,[4]
K. Hagel,[1] J. Gauthier,[1] S. Ota,[5] A. Richards,[6] and S. J. Yennello[1,2,3]
[1]*Cyclotron Institute, Texas A&M University, College Station, TX 77843*
[2]*Department of Chemistry, Texas A&M University, College Station, TX 77843*
[3]*Department of Physics, Texas A&M University, College Station, TX 77843*
[4]*Los Alamos National Laboratory, Los Alamos, NM 87545*
[5]*Brookhaven National Laboratory, Upton, NY 11973*
[6]*Ohio University, Athens, OH 45701*

The photon strength function (PSF) is a statistical property of the nucleus describing gamma-ray emission probabilities and is an essential quantity for calculating neutron-capture cross sections within the Hauser-Feshbach formalism. It has been shown to exhibit a low-energy enhancement (LEE) at low gamma-ray energies for other iron isotopes (^{56,57}Fe) from previous measurements [1,2,3] which could have significant impact in nucleosynthesis [4]. Due to the importance of these reactions for nuclear astrophysics, nuclear waste transmutation, and nuclear energy and the difficulty of direct measurements on short-lived nuclei, the Detector Array for Photons, Protons, and Exotic Residues (DAPPER) [5] was constructed to make measurements of the statistical properties of nuclei using indirect methods. Using the (d,p) reaction in inverse kinematics, the PSF for ^{58}Fe was extracted from particle-gamma coincidence data obtained using an S3 annular silicon detector and 128 BaF_2 scintillators to determine the excitation energy from the emitted proton and the gamma-ray energies, respectively. The Oslo method provides both the PSF and the nuclear level density (NLD) using a normalization procedure [6] while the Shape method provided a functional form of the PSF in a model-independent way [7]. Four separate coincidence matrices are explored: (a) excitation energy versus crystal gamma-ray energies, (b) excitation energy versus cluster gamma-ray energies (Compton add-back routine), (c) excitation energy versus crystal gamma-ray energies in events with total gamma-ray energy collection (total sum gate TSG), and (d) excitation energy versus cluster gamma-ray energies with the TSG.

Following the procedure for the Oslo methods, the raw particle-gamma coincidence data was unfolded [8] using the detector response generated with GEANT4 and then an iterative subtraction procedure was implemented [9] to extract the first-generation gamma-rays. The Oslo method proceeds with a chi-square fit across a statistical region of the primary matrix [6] to obtain functional forms of the NLD and PSF which are then constrained using the known discrete level density, the s-wave neutron level spacing parameter at the neutron separation energy ($D_0(S_n)$) and the average s-wave radiative width at the neutron separation energy ($\langle \Gamma_\gamma \rangle(S_n)$). Two separate statistical regions were explored, both sharing excitation energy cuts from 5.5-9.5 MeV and one with a low gamma-ray energy region at 3.5 MeV and another at 2.0

MeV. Given possible issues originating from over-subtractions resulting from strongly populated states at low excitation energies, the 2 MeV gamma-ray cuts are not discussed further here [10]. Fig. 1 shows the extracted NLDs from the Oslo method; panels (a) and (b) agree well with the known level density for ^{58}Fe and join smoothly with a constant temperature (CT) model interpolation from the calculated level density at the separation energy ($\rho(S_n)$). The data in panels (c) and (d) using the TSG show an over-estimate of the low-energy discrete regions possibly resulting from the preferential selection on low multiplicity events. The total error bands

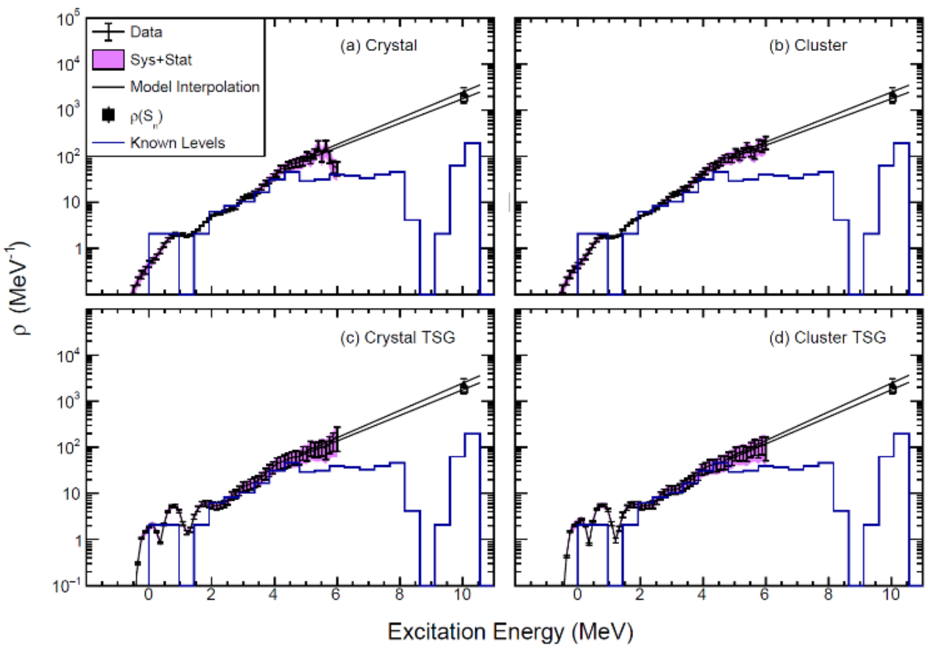

FIG.1. NLDs obtained from the Oslo analysis on each of the coincidence matrices. The known levels are indicated by the binned blue line, the calculated $\rho(S_n)$ by the points, and the CT model interpolation as the thin black line. The two calculated $\rho(S_n)$ are determined using separate models and make up upper and lower bounds.

include systematic errors originating from reported uncertainties in the previously mentioned normalization parameters. The extracted PSF in Fig. 2 panel (a) agrees well with two theoretical predictions (QRPA and SMLO [11]) while panels (b), (c), and (d) appear to possess lower strength at lower gamma-ray energies. This discrepancy could result from uncertainties in the unfolding and primary methods not properly accounting for the impact of the clustering algorithm and the TSG.

The Shape methods proceeds with a selection of two final state populations in the primary matrix, in this case the 810 and 1675 keV first and second excited states. These two states are both 2^+ which simplifies the calculation. The TSG matrices provide clear final state diagonals in the primary matrices and so are the focus of the Shape method analysis. For each excitation energy bin in the statistical region (5.5-

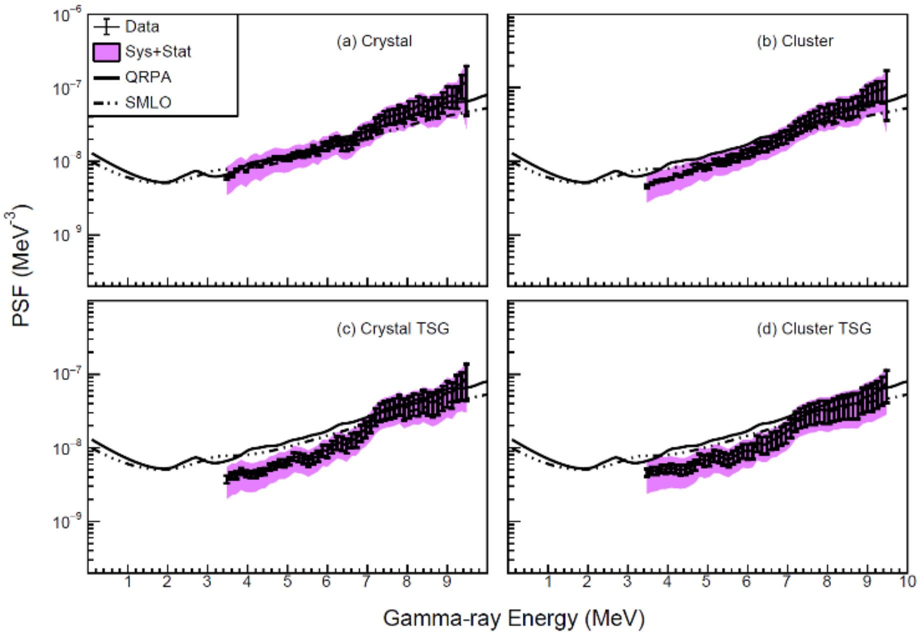

FIG. 2. PSFs obtained from the Oslo analysis for each of the coincidence matrices. The solid and dotted-dashed black lines are two theoretical predictions for the PSF of ^{58}Fe.

9.5 MeV) the strength can be estimated by the yield of primary gamma-rays and an internal normalization provides a functional shape of the PSF for ^{58}Fe. This method requires no constraint to external data. A scaling of the PSF acquired from the Shape method can then be compared to the results from the Oslo method and has been done so in Fig. 3. The agreement is very good with the crystal data, and slightly in

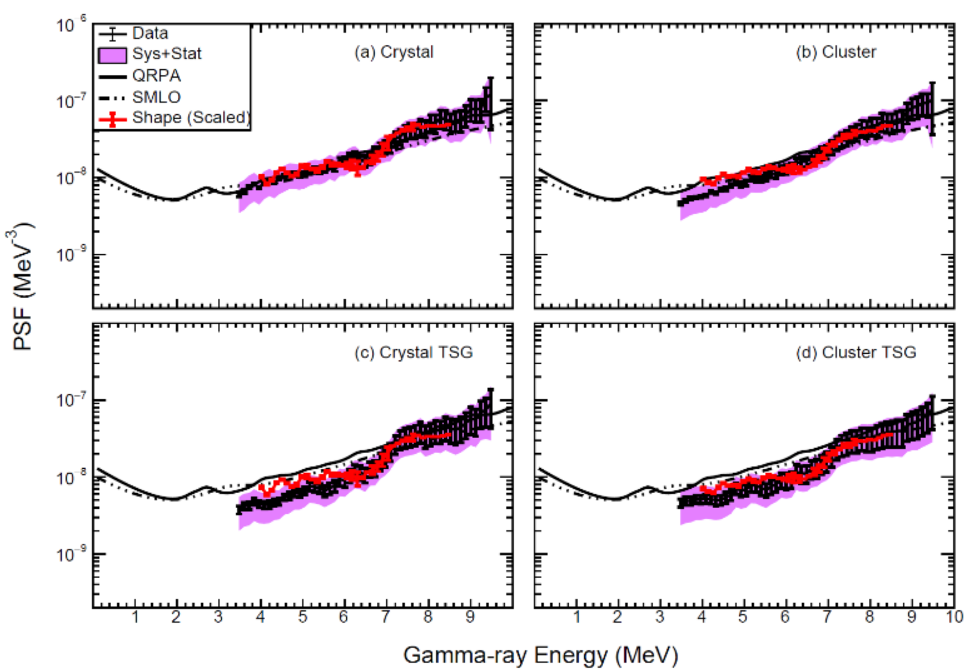

FIG. 3. Same Oslo PSFs from Figure 2, but with the Shape method results added (red points). Very good agreement is achieved in panel (a). Slight low-energy discrepancies for panels (b), (c), and (d) may arise from uncertainties associated with the clustering and TSG

disagreement at lower gamma-ray energies compared to the data in panels (b), (c), and (d) likely for the reasons previously mentioned. Given the good agreement between the crystal data Oslo PSF with the Shape method PSF obtained from a separate matrix, it is then compared to the previously measured Oslo iron data in Fig. 4. The agreement in slope and magnitude is quite good. No LEE is reported in ^{58}Fe in this data set given the presence of strongly populated low-energy excited states.

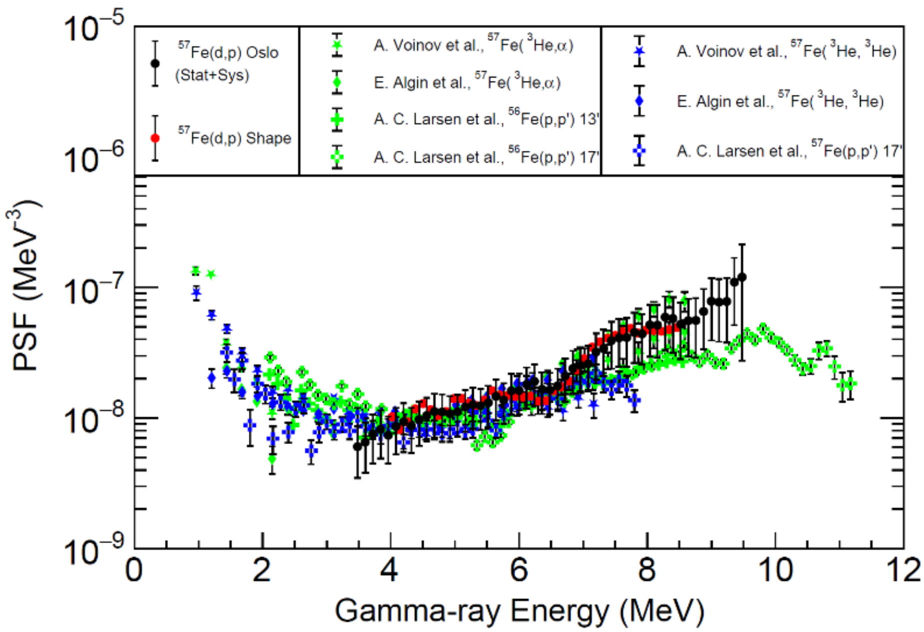

FIG. 4. Crystal results from this data set (black (Oslo) and red (Shape) points) compared to previous Oslo method measurements on 56,57Fe. For the 58Fe data, systematic errors are included. In the previous measurements only statistical errors are reported. Consistent magnitude and slope are obtained, though a LEE is not probed in this work due to the presence of systematic issues (see text).

[1] A. Voinov *et al.*, Phys. Rev. Lett. **93**, 142504 (2004).

[2] E. Algin *et al.*, Phys. Rev. C **78**, 054321 (2008).

[3] A.C. Larsen *et al.*, Phys. Rev. Lett. **111**, 242504 (2013).

[4] A.C. Larsen and S. Goriely, Phys. Rev. C **82**, 014318 (2010).

[5] A.B. McIntosh, M. Sorensen, and A. Abbott, Nucl. Instrum. Methods Phys. Res. A (in preparation).

[6] A Schiller *et al.,* Nucl. Instrum. Methods Phys. Res. **A447**, 498 (2000).

[7] M. Wiedeking, M. Guttormsen, A.C. Larsen, F. Zeiser, A. Görgen, S.N. Liddick, D. Mücher, S. Siem, and A. Spyrou, Phys. Rev. C **104**, 014311 (2021).

[8] M. Guttormsen, T.S Tveter, L Bergholt, F Ingebretsen, and J Rekstad, Nucl. Instrum. Methods Phys. Res. **A374**, 371 (1996).

[9] M. Guttormsen, T. Ramsøy, and J. Rekstad, Nucl. Instrum. Methods Phys. Res. **A255**, 518 (1987).

[10] A. Abbott, PhD Thesis, Texas A&M University, 2024.

[11] S. Goriely *et al.*, Eur. Phys. J. A **55**, 172 (2019).